American Mineralogist, Volume 65, pages 313-320, 1980

Composition and cation order variations in a sector-zoned blueschist pyroxene

MICHAEL A. CARPENTER

Hoffman Laboratory, Department of Geological Sciences
Harvard University, Cambridge, Massachusetts 02138

Abstract

Pyroxene crystals in almost monomineralic veins cutting a blueschist rock from California show sector zoning. Portions of each crystal which grew at faces cutting the *c* axis are sodic augite (*e.g.* $Jd_{11}Ac_{20}Aug_{69}$) whereas omphacite (*e.g.* $Jd_{35}Ac_{18}Aug_{47}$) formed at faces parallel to the *c* axis (probably at {100}, {010}, {110}). Examination by transmission electron microscopy reveals that the omphacite has a primitive lattice with antiphase domains on a scale of less than ~50Å and, in a few areas, exsolution lamellae approximately parallel to (100) of a disordered pyroxene. The sodic augite contains fine lamellae of amphibole (?) approximately parallel to (010).

I suggest that the activities of ions in the solutions from which crystallization occurred dictated a pyroxene composition between omphacite and augite but that this lay within a broad, low-temperature miscibility gap and two pyroxenes grew simultaneously. The sectoral arrangement developed during rapid crystal growth; local charge balance effects in each new layer of material controlled the composition distribution. Short-range ordering occurred during growth in directions normal to the pyroxene chains (giving omphacite) but was restricted during growth parallel to the chains (giving sodic augite).

Introduction

Sector zoning is well known in minerals. The phenomenon is of special interest in that variations in composition between different sectors of individual crystals reflect local variations in crystal growth conditions and therefore provide an insight into the factors controlling the formation of minerals. Although there appear to be as many theories to explain the origin of sector zoning as there are examples of it, most authors agree that it develops under metastable conditions where growth rates are too rapid for bulk equilibration between crystals and their growth medium. The best documented cases are reviewed by Dowty (1976) and include titanaugite, staurolite, and augite/pigeonite.

Possible causes of sector zoning can be divided into two categories: control by the supply of ions to the growth surface and control by the structure of the crystal faces. If the rate of arrival of ions to the surface is inadequate to keep up with the crystal growth rate, then extraneous ions will be metastably incorporated. Because crystal faces not related by symmetry tend to grow at different rates, growth zones will develop which depart from the equilibrium composition to differing extents (Leung, 1974). If the most important constraint is the structure of the exposed crystal faces, then a number of factors can influence the observed composition distribution. These include: (a) the nature of partially formed cation sites on the surface, "protosites" (Nakamura, 1973; Dowty, 1976), at which cations can be adsorbed and then incorporated in non-equilibrium proportions into the crystal; (b) the need to maintain charge balance within each layer or between successive layers of deposited material, as for $Al^{vi} + 2Al^{iv} \rightleftarrows H^+ + 2Si$ substitutions in staurolite (Hollister, 1970); (c) the presence of a solvus and the orientation of best-fitting crystal planes for epitaxial overgrowths, as in augite/pigeonite (Bence and Papike, 1971; Hollister *et al.*, 1971; Boyd and Smith, 1971). Differences between growth sectors need not be restricted simply to composition. The degree of cation or anion order can also vary, as in adularia (Akizuki and Sunagawa, 1978), topaz (Akizuki *et al.*, 1979), and some staurolites (Dollase and Hollister, 1969).

In this paper a new example of sector zoning, involving sectors of sodic augite and omphacite, is described. The crystals appear to have grown rapidly in a low-temperature (blueschist facies) metamorphic

0003-004X/80/0304-0313$02.00

rock and have both compositional and order differences between their sectors. A complete explanation of the crystal growth mechanisms cannot be offered but several of the constraints discussed above may be involved. For example, charge-balancing problems are thought to affect the distribution of R^{+}, R^{2+}, R^{3+} cations in ordered omphacite (Clark *et al.*, 1969), and there is the possibility of a miscibility gap between omphacite and sodic augite (Brown *et al.*, 1978).

Cation ordering in omphacite leads to a symmetry reduction from a C-face-centered to a primitive lattice (Clark and Papike, 1968) and the appearance of antiphase domains (APD's) observable by transmission electron microscopy (Champness, 1973; Phakey and Ghose, 1973). Champness argues that natural omphacites grow metastably in a disordered (or partially ordered) state below their equilibrium ordering temperature (T_{ord}) and then order, whereas Yokoyama *et al.* (1976) favor a low value of T_{ord} and APD formation during cooling. Fleet *et al.* (1978) demonstrated that T_{ord} may be as high as 725±20°C, well above the crystallization temperature of most omphacites, but suggested that the APD's are a growth feature. There is still disagreement therefore about whether natural omphacites grow with metastable limited order (Champness, 1973; Carpenter, 1978) or with a high degree of long-range order (Fleet *et al.*, 1978).

Specimen description and observations

The sodic pyroxenes occur in emerald green veins up to 1 cm wide in a glaucophane–epidote–muscovite–sphene schist. The hand specimen was collected by Dr. S. O. Agrell as a loose block in a landslip of low-grade Franciscan rocks at Russian River, seven miles north of Cloverdale, California (Harker collection no. 102729, Dept. of Mineralogy and Petrology, Cambridge, England). It closely resembles the samples figured by Essene and Fyfe (1967) except that the pyroxene crystals have no obvious preferred orientations. The veins consist of 99% pyroxene with rare quartz and muscovite. Individual crystals are composite and have roughly tabular shape with dimensions ~1mm × 1mm × 0.5mm with the short dimension parallel to the *c* axis. In most orientations, with the notable exception of two cleavage sections, they show a distinctive hour-glass texture (Fig. 1). They do not extinguish uniformly between crossed polars but appear to be slightly curved. The pyroxene cleavages show similar curvature. There are some variations of the typical hour-glass texture, particularly at the sector interfaces where one sector may branch into the other.

Due to the interlocking of the crystals, growth faces have only rarely been preserved. There are occasional pockets of quartz into which protruding pyroxene crystals have straight or slightly curved faces (Fig. 1a). These crystals appear to have grown into cavities which were later filled by quartz, and their growth faces lie parallel to the *c* axis and at steep angles to it. The most common growth habit of pyroxene crystals includes {110}, {100}, {010}, which are almost certainly developed in this case, and $\{11\bar{1}\}$ as the faces cutting the *c* axis. $\{11\bar{1}\}$ faces would give more sharply pointed terminations to the crystals than are observed, but other known possibilities, such as {011}, $\{\bar{1}01\}$, and {001}, do not appear to give the observed interfacial angles either and positive identification of the terminal faces has not been made. Growth normal to the *c* axis (presumably at {100}, {010}, {110} faces) was of omphacite, whereas in the *c* direction sodic augite formed. The sodic augite portions have fine lamellar features parallel to the cleavage (Fig. 1c), which makes a useful contrast with the omphacite for optical identification purposes.

Electron probe analysis

The methods of analysis and recalculation are the same as discussed by Carpenter (1979a). For the estimation of Fe^{2+}/Fe^{3+} proportions it was assumed that Si = 2.00 because the analyses show a slight excess of silica (possibly due to a systematic error; see Carpenter, 1979a). Fe^{3+} was then taken as Na − Al, and proportions of jadeite, acmite and augite molecules were recalculated to a total of 100% from Jd = Al, Ac = Fe^{3+}, Aug = Ca. Representative analyses are shown in Table 1 and all the data are plotted in Figure 2.

There is a sharp compositional break between the sectors (Fig. 2). The *c*-axis sectors have 8–15% jadeite while the central omphacite portions have 28–41% jadeite. No systematic zoning was detected within the sectors. Small pyroxene crystals in the host glaucophane schist have compositions in the same range as the vein omphacite (Fig. 2).

Electron microscopy

Specimens were prepared for transmission electron microscopy by ion beam thinning and were examined in an AEI EM6G microscope operating at 100kV. The crystals contained a high density of defects, such as dislocations, which may account for their non-uniform optical extinction.

Selected area diffraction (SAD) patterns from homogeneous omphacite regions contained diffuse h + k = odd reflections, indicating a P lattice and cation

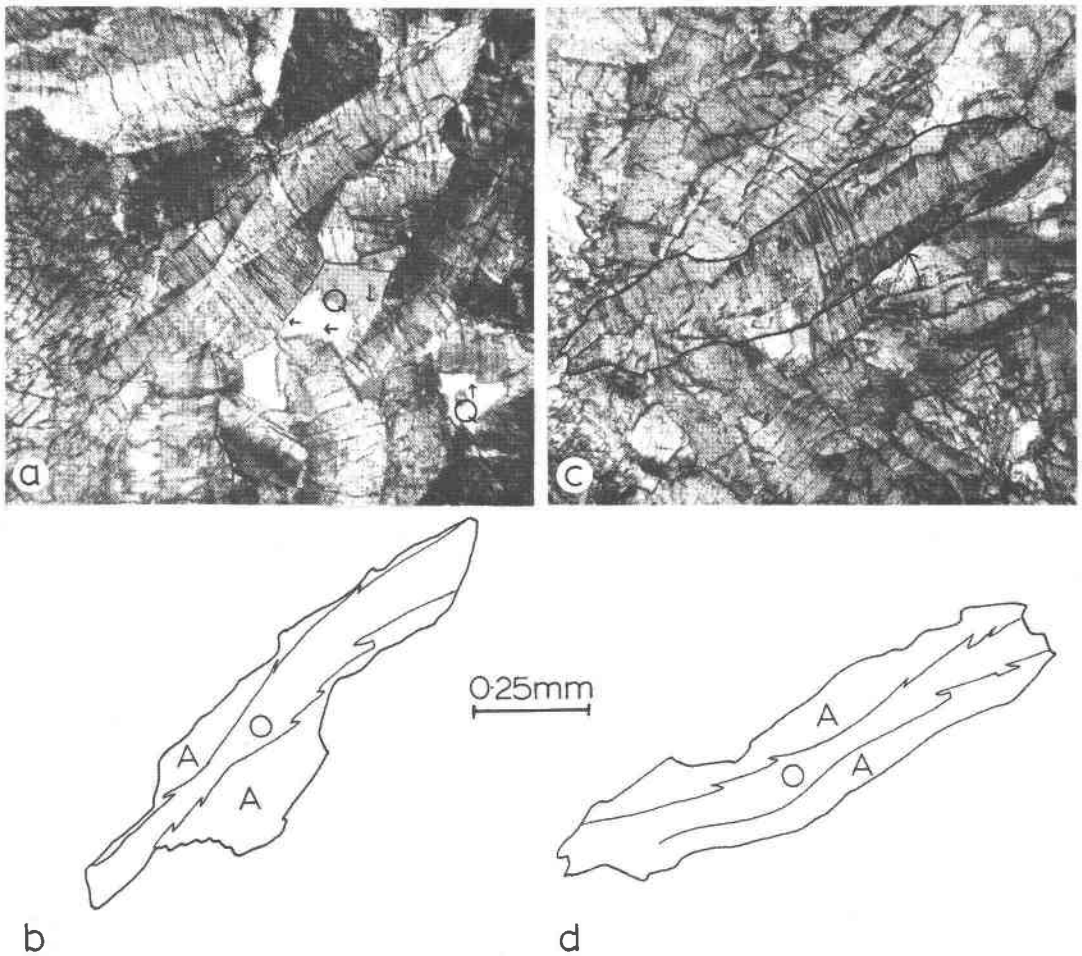

Fig. 1. Optical micrographs of sector-zoned vein pyroxene crystals (partially crossed polars). (a) Hour-glass texture of omphacite and sodic augite. Slightly curved crystal faces and some surface ledges (arrowed) can be seen against quartz (Q). (b) Sketch of zoned crystal in (a) showing the branching sector interfaces. A = augite, O = omphacite. (c) Sector zoned crystal with fine lamellae in the sodic augite (arrowed). (d) Sketch of (c).

ordering. The maximum size of equiaxed APD's which could be imaged using these reflections was ~50Å (Fig. 3a), but in general they were below the resolution limits of the electron microscope. A few areas with coarser, highly irregular domains were observed. SAD patterns from sodic augite had absences appropriate for a C-face-centered lattice (h + k = odd reflections absent).

Exsolution, in the form of fine (~100Å) composition modulations approximately parallel to (100), was found in patches (Fig. 3b). Dark-field images with h + k = odd reflections show one component in contrast and the other out, suggesting that one is ordered and the other is not. This microstructure is discussed in more detail elsewhere in relation to the general problem of exsolution in sodic pyroxenes (Carpenter, 1979b). SAD patterns showing a^*–c^* sections from exsolved and homogeneous areas of omphacite typically have weak violations of an *n* glide parallel to (010), suggesting that the space group of the ordered structure may be $P2$ as opposed to $P2/n$.[1]

Sodic augite regions frequently contain fine lamellae approximately parallel to (010) (Fig. 3c) which may correspond to the lamellar features observed optically. SAD patterns from these areas have considerable streaked intensity along the b^* direction

[1] Clark and Papike (1968) and Clark *et al.* (1969) reported a $P2$ space group for ordered omphacite, but subsequent authors (Matsumoto *et al.*, 1975; Curtis *et al.*, 1975) have argued in favor of $P2/n$. Weak *n*-glide violations have, however, been observed in selected area electron diffraction patterns from several specimens, particularly where the APD size is small (Carpenter, 1978, 1979a; Carpenter and Okay, 1978).

Table 1. Representative pyroxene analyses. Aug1 and Om1 are from sodic augite and omphacite sectors of a single crystal. Aug2 and Om2 are from a second crystal and Aug3, Om3 from a third

Analysis no.	Aug1	Om1	Aug2	Om2	Aug3	Om3
SiO_2	53.97	55.26	54.03	55.55	54.09	55.41
Al_2O_3	2.38	8.19	1.52	9.00	2.42	7.72
FeO *	11.05	9.73	10.81	9.64	10.54	10.43
MnO	0.29	0.18	0.33	0.21	0.19	0.00
MgO	9.61	5.78	9.77	5.02	9.56	5.73
CaO	17.22	11.76	18.63	10.64	18.36	11.82
Na_2O	4.36	7.51	3.41	8.30	3.72	7.47
Total	98.88	98.41	98.50	98.36	98.88	98.58
Cations per 2.00 Si						
Si^{4+}	2.00	2.00	2.00	2.00	2.00	2.00
Al^{3+}	0.11	0.35	0.07	0.38	0.11	0.33
Fe^{3+} **	0.20	0.18	0.17	0.20	0.16	0.20
Fe^{2+}	0.14	0.12	0.16	0.09	0.17	0.11
Mn^{2+}	0.01	0.01	0.01	0.01	0.01	0.00
Mg^{2+}	0.53	0.31	0.54	0.27	0.53	0.31
Ca^{2+}	0.69	0.46	0.74	0.41	0.73	0.46
Na^{+}	0.31	0.53	0.24	0.58	0.27	0.53
ΣM	3.99	3.96	3.93	3.94	3.98	3.94
Jd	11	35	7	38	11	33
Ac	20	18	17	20	16	20
Aug	69	47	76	42	73	47

* Total Fe given as FeO
** Fe^{3+} calculated as Na - Al
Trace amounts of Cr_2O_3, V_2O_3, TiO_2 detected in some crystals
NiO, K_2O not detected

but apparently with positions of maximum intensity (Fig. 3d). The diffraction patterns are similar to those arising from exsolution lamellae of amphibole parallel to (010) in augite (Smith, 1977). In the present specimen the lamellae are tentatively identified as amphibole, but it is not clear whether they formed by exsolution or alteration.[2]

Discussion

Essene and Fyfe (1967) and Coleman and Clark (1968) estimated $T \sim 200$–300°C and $P \sim 6$–9kbar for the formation of the California blueschists, but higher temperatures have been proposed for the high-grade tectonic blocks, some of which contain blueschist assemblages (Taylor and Coleman, 1968). Essene *et al.* (1965) suggested that the occurrence of epidote, as in the specimen described here, rather than lawsonite, does not necessarily indicate higher metamorphic temperatures and that the temperature of vein formation may also have been in the vicinity of 300°C.

The curvature of pyroxene crystals and their high density of defects are probably growth features because the veins show no obvious signs of deformation. This implies rapid crystal growth. The sectoral arrangement of sodic augite and omphacite cannot easily be explained as overgrowth or replacement during crystallization of successive phases, as for example can the omphacite rims on impure jadeite from the Urals (Dobretsov and Ponomareva, 1968), and from Guatemala and Syros (Carpenter, 1978, 1979a). Simultaneous crystallization of two pyroxene compositions is also compatible with the interfingering interfaces between some sectors (Fig. 1a). Omphacite appears to have grown on faces parallel to the *c* axis whereas sodic augite grew on faces cutting the *c* axis. In places small surface ledges can be seen which expose both types of face (Fig. 1a). Deposition of successive layers of the preferred phase at each face would lead to the observed branching sector boundaries (Fig. 4).

The hiatus in composition between sectors is most readily explained if there is a miscibility gap between sodic augite and omphacite at low temperatures, as in the case of augite/pigeonite sectoral intergrowths where the solvus is between Ca-rich and Ca-poor compositions. Such a miscibility gap has already been suggested by Brown *et al.* (1978), who described an apparent equilibrium coexistence of slightly manganese-enriched omphacite and diopside. As these authors pointed out, however, it is frequently difficult to discriminate between equilibrium and metastable assemblages in low-temperature metamorphic rocks. There is more substantial evidence for limited miscibility between jadeite and omphacite at low temperatures (Dobretsov *et al.*, 1971; Carpenter, 1979a), and consideration of the ionic radii of the M-site cations supports the argument that non-ideal solid solution behavior should occur in the whole range jadeite (Na^+, 1.02Å; Al^{3+}, 0.54Å)–diopside (Ca^{2+}, 1.00Å; Mg^{2+}, 0.72Å). Deviations from ideality will be enhanced by the substitution of Fe^{2+} (0.78Å) for Mg^{2+} but reduced by the substitution of Fe^{3+} (0.65Å) for Al^{3+} (ionic radii from Shannon, 1976). In the absence of cation ordering at intermediate compositions (*i.e.* primitive omphacite), a solvus might be anticipated between jadeite and augite at low tem-

[2] Fine lamellae of what appear to be amphibole have also been observed in aegirine–jadeite from a Syros blueschist (Carpenter, unpublished data). Coleman and Clark (1968) reported X-ray evidence for amphibole intergrown with a jadeite from California.

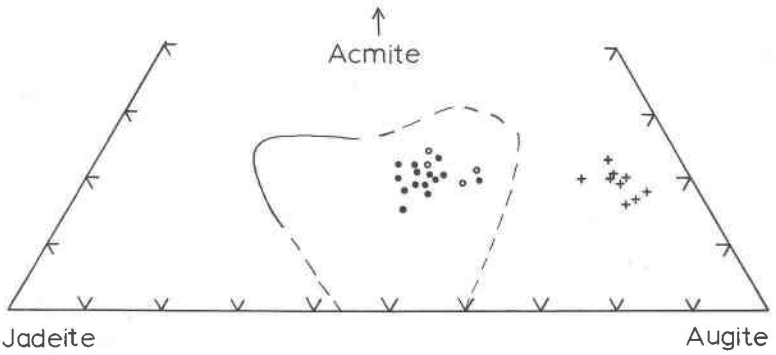

Fig. 2. Electron microprobe analyses of pyroxenes from 102729. Each point is one analysis. Crosses are from *c*-axis sectors and filled circles from other sectors of vein crystals. Open circles are groundmass pyroxenes. The continuous and broken lines represent the composition limits of cation ordering observed in blueschist omphacites (from Carpenter, 1979a).

peratures.[3] If so, then omphacite may only appear in low-temperature rocks if it grows with some degree of cation order to stabilize it relative to the two-phase end-member assemblage. The TEM observations indicate that the maximum scale of long-range order in the omphacite described here is ~50Å, but is generally much less, so that cation ordering achieved during growth can only have been limited and short range in character.

Constraints on sector zoning

The activities of ions in the migrating solutions from which the vein crystals grew apparently dictated that a pyroxene intermediate in composition between omphacite and sodic augite should form. However, this composition lay within a miscibility gap and the simultaneous crystallization of two phases separated by 15–20% jadeite content resulted. The question remains as to why the two phases grew as different sectors of single crystals. The constraints which apply to other examples of sector zoning, as discussed in the introduction, can each be considered. Firstly the growth rate was rapid but the supply of ions to the growth surfaces does not seem to have been a problem because there is no systematic zoning within the sectors. The important factors must relate to differences in crystal structures between faces parallel to or cutting the *c* axis.

(a) Adsorption at protosites. According to the models of Nakamura (1973) and Dowty (1976), the most flexible M1 and M2 protosites in pyroxenes are at {100} faces. The cations which should be adsorbed preferentially at these sites are those which can form the strongest bonds, *i.e.* those with the largest charge and smallest ionic radii (Dowty, 1976). Of the cations available, Al^{3+} on M1 and Ca^{2+} on M2 should be incorporated in preference to Mg^{2+} and Na^{+}, respectively. To maintain charge balance these would have to be accompanied by equivalent proportions of Na and Mg, giving omphacite (Fe^{2+} is expected to follow Mg, and Fe^{3+} to follow Al^{3+}). Protosites on {010}, {110}, {11$\bar{1}$}, (and {001}) faces have more complete oxygen coordination but are similar to each other. A protosite model would therefore predict the largest difference in sector compositions to be between {100} and the rest. This is not the case in the present specimen.

(b) Charge balancing. The charge differences between cations in omphacite play a critical role in determining the ordered configuration (Clark *et al.*, 1969). M1 sites in chains parallel to *c* are occupied alternately by Mg and Al and M2 sites are filled predominantly by Ca or Na, according to whether two of the three M1 cations with which they share oxygens are Mg or Al respectively[4] (Clark *et al.*, 1969; Curtis *et al.*, 1975; Matsumoto *et al.*, 1975). Because the low crystallization temperatures were almost certainly below T_{ord}, there must have been a tendency for ordering to occur at the earliest possible opportunity, and it has already been suggested that limited short-range order was incorporated into the growing omphacite sectors. Omphacite may therefore have

[3] A similar solvus was proposed by Bell and Davis (1965) but at high temperatures. Their experimental results, however, conflict with those of Kushiro (1964) obtained under approximately similar conditions and have not been substantiated.

[4] It is assumed that the ordering follows essentially *P2/n* symmetry and that the weak *n*-glide violations observed in electron diffraction patterns in this case represent only minor departures from this.

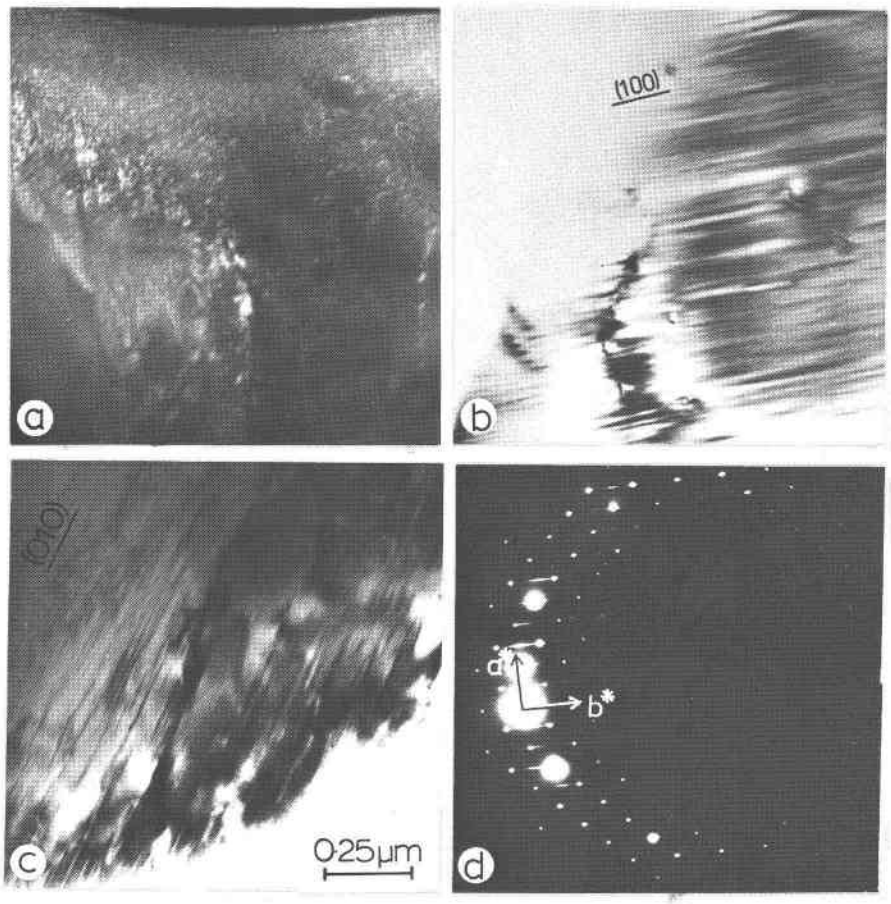

Fig. 3. Electron micrographs of vein pyroxenes. (a) Antiphase domains in an omphacite sector. Dark field using an h + k = odd reflection. (b) Fine composition modulations approximately parallel to (100) in omphacite; bright field. (c) Fine lamellae approximately parallel to (010) of (?) amphibole in sodic augite; bright field. (d) Electron diffraction pattern from an area similar to (c). The streaked reflections are from the lamellae. (a), (b), (c) are at the same magnification.

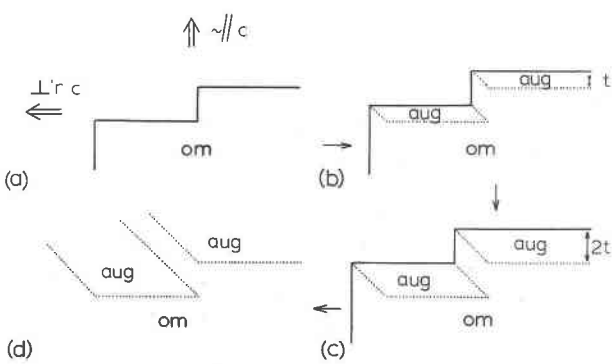

Fig. 4. Schematic two-dimensional cross section through a crystal to illustrate the effect of a ledge (shown in a) at the growth faces. Successive layers (with thickness t) on faces growing perpendicular to the *c* axis are of omphacite (shaded) but are sodic augite on faces growing in the *c* direction (unshaded) (b,c). The result is a branched sector interface (dotted line) (d).

formed at the faces most favorable for ordering in the surface layer, and conversely sodic augite may have grown where ordering in the layer being deposited was most difficult. At {100} faces alternate M1 sites in the octahedral chains are simultaneously exposed, allowing Mg^{2+} to be adsorbed preferentially next to Al^{3+}. Almost the same situation arises at {110} and {010} except that the M1 sites are not quite coplanar. Adjacent M2 sites within the layers and in successive layers can be filled according to the charge balance requirements. The situation at {001}, however, forms a sharp contrast. The cation occupying an M1 site in a new (001) layer would be influenced by an M2 cation immediately next to it. In the ordered omphacite structure these sites must be filled by Mg and, on average, 1/3Ca 2/3Na (or Al and 1/3Na 2/3Ca). Thus in most cases Mg^{2+} is next to Na^{+} and Al^{3+} next to Ca^{2+}, giving a local charge deficiency or excess.

These charge imbalances within the new (001) layer would act in opposition to cation ordering during growth. The same applies to other faces cutting the *c* axis, but the effect decreases as they make a steeper and steeper angle to it. A requirement of both short-range ordering and local charge balance in the growth layers therefore can only be met at faces parallel to *c*, where omphacite develops. Ordering and charge balancing are less compatible at the faces cutting *c*, so that the growth of augite is preferred.

(c) Nucleation and epitaxial growth. If original omphacite nuclei acted as nucleation sites for sodic augite, or *vice versa*, the shared plane should be the one with best structural match. From the exsolution relations of the ordered and disordered components (Fig. 3b), this appears to be (100) and not a plane at an angle to the *c* axis. A further reason for rejecting this explanation is that the choice of growth planes was not restricted to the earliest stages of crystallization. The two phases grew on their preferred faces at surface ledges even during the later stages of crystal growth, leading to the branching texture of some of the sector interfaces.

The most satisfactory explanation for the sector zoning involves local charge balancing within each new layer of material being deposited combined with a tendency for cation ordering to occur at the earliest possible stages of crystal growth. This mechanism is broadly similar to that proposed for sector zoning in staurolite by Hollister (1970), though for the present case there is probably the additional effect of a miscibility gap between omphacite and sodic augite.

Conclusions

Sector zoning in sodic pyroxenes from Cloverdale, California developed during rapid crystal growth and involved differences of both composition and cation order. The main constraint on sector formation appears to have been the need to maintain local charge balance within the growth layers so that cation ordering during growth was possible only at faces parallel to the *c* axis. The intergrown crystals provide supporting evidence for a low-temperature miscibility gap between omphacite and sodic augite. The omphacite represents the first case where it can be positively stated that reasonable-sized antiphase domains (larger than a few unit cells) did not form during growth below T_{ord}. Rather, metastable growth with limited short-range cation ordering seems to have occurred.

Acknowledgments

I am grateful to Dr. S. O. Agrell for providing the specimen and to Dr. D. L. Bish, Dr. C. Klein, Dr. L. S. Hollister, and Dr. E. J. Essene for criticisms of and improvements to the manuscript. I acknowledge the receipt, from The Natural Environment Research Council of Great Britain, first of a Research Studentship held at the Department of Mineralogy and Petrology, Cambridge University, England, and lately of a Research Fellowship.

References

Akizuki, M. and I. Sunagawa (1978) Study of the sector structure in adularia by means of optical microscopy, infra-red absorption, and electron microscopy. *Mineral. Mag., 42,* 453–462.

———, M. S. Hampar and J. Zussman (1979) An explanation of anomalous optical properties of topaz. *Mineral. Mag., 43,* 237–241.

Bell, P. M. and B. T. C. Davis (1965) Temperature–composition section for jadeite–diopside. *Carnegie Inst. Wash. Year Book, 64,* 120–123.

Bence, A. E. and J. J. Papike (1971) A martini-glass clinopyroxene from the moon. *Earth Planet. Sci. Lett., 10,* 245–251.

Boyd, F. R. and D. Smith (1971) Compositional zoning in pyroxenes from lunar rock 12021, Oceanus Procellarum. *J. Petrol., 12,* 439–464.

Brown, P., E. J. Essene and D. R. Peacor (1978) The mineralogy and petrology of manganese rocks from St. Marcel, Piedmont, Italy. *Contrib. Mineral. Petrol., 67,* 227–232.

Carpenter, M. A. (1978) Kinetic control of ordering and exsolution in omphacite. *Contrib. Mineral. Petrol., 67,* 17–24.

——— (1979a) Omphacites from Greece, Turkey and Guatemala: composition limits of cation ordering. *Am. Mineral., 64,* 102–108.

——— (1979b) Mechanisms of exsolution in sodic pyroxenes. *Contrib. Mineral. Petrol.* (accepted for publication).

——— and A. Okay (1978) Topotactic replacement of augite by omphacite in a blueschist rock from north-west Turkey. *Mineral. Mag., 42,* 435–438.

Champness, P. E. (1973) Speculation on an order–disorder transformation in omphacite. *Am. Mineral., 58,* 540–542.

Clark, J. R. and J. J. Papike (1968) Crystal-chemical characterization of omphacites. *Am. Mineral., 53,* 840–868.

———, D. E. Appleman and J. J. Papike (1969) Crystal-chemical characterization of clinopyroxenes based on eight new structure refinements. *Mineral. Soc. Am. Spec. Pap., 2,* 31–50.

Coleman, R. G. and J. R. Clark (1968) Pyroxenes in the blueschist facies of California. *Am. J. Sci., 266,* 43–59.

Curtis, L. W., J. Gittins, V. Kocman, J. C. Rucklidge, F. C. Hawthorne and R. B. Ferguson (1975) Two crystal structure refinements of a *P2/n* titanian ferro-omphacite. *Can. Mineral., 13,* 62–67.

Dobretsov, N. L., Yu. G. Lavrent'yev and L. N. Pospelova (1971) Immiscibility in Na–Ca pyroxenes. *Dokl. Akad. Nauk. SSSR, 201,* 152–155.

——— and L. G. Ponomareva (1968) Comparative characteristics of jadeite and associated rocks from Polar Urals and Prebalkash region. *International Geol. Rev., 10,* 221–242, 247–279.

Dollase, W. A. and L. S. Hollister (1969) X-ray evidence of ordering differences between sectors of a single staurolite crystal. *Geol. Soc. Am. Abstracts with Programs, 7,* 268–270.

Dowty, E. (1976) Crystal structure and growth: II. Sector zoning in minerals. *Am. Mineral., 61,* 460–469.

Essene, E. J. and W. S. Fyfe (1967) Omphacite in Californian metamorphic rocks. *Contrib. Mineral. Petrol., 15,* 1–23.

———, ——— and F. J. Turner (1965) Petrogenesis of Franciscan glaucophane schists and associated metamorphic rocks. *Contrib. Mineral. Petrol., 11,* 695–704.

Fleet, M. E., C. T. Herzberg, G. M. Bancroft and L. P. Aldridge (1978) Omphacite studies, I: The $P2/n \rightarrow C2/c$ transformation. *Am. Mineral., 63,* 1100–1106.

Hollister, L. S. (1970) Origin, mechanisms and consequences of compositional sector-zoning in staurolite. *Am. Mineral., 55,* 742–766.

———, W. E. Trzcienski Jr., R. B. Hargraves and C. G. Kulick (1971) Petrogenetic significance of pyroxenes in two Apollo 12 samples. *Proc. 2nd. Lunar Sci. Conf,* 259–557.

Kushiro, I. (1965) Clinopyroxene solid solutions at high pressures. *Carnegie Inst. Wash. Year Book, 64,* 112–117.

Leung, I. S. (1974) Sector zoned titanaugites: morphology, crystal-chemistry and growth. *Am. Mineral., 59,* 127–138.

Matsumoto, T., M. Tokonami and N. Morimoto (1975) The crystal structure of omphacite. *Am. Mineral., 60,* 634–641.

Nakamura, Y. (1973) Origin of sector zoning of igneous clinopyroxenes. *Am. Mineral., 58,* 986–990.

Phakey, P. P. and S. Ghose (1973) Direct observation of antiphase domain structure in omphacite. *Contrib. Mineral. Petrol., 39,* 239–245.

Shannon, R. D. (1976) Revised effective ionic radii and systematic studies of interatomic distances in halides and chalcogenides. *Acta Crystallogr., A32,* 751–767.

Smith, P. P. K. (1977) An electron microscope study of amphibole lamellae in augite. *Contrib. Mineral. Petrol., 59,* 317–322.

Taylor, H. P. and R. G. Coleman (1968) O^{18}/O^{16} ratios of coexisting minerals in glaucophane-bearing metamorphic rocks. *Geol. Soc. Am. Bull., 79,* 1727–1756.

Yokoyama, K., S. Banno and T. Matsumoto (1976) Compositional range of $P2/n$ omphacite from the eclogitic rocks of Central Shikoku, Japan. *Mineral. Mag., 40,* 773–779.

Manuscript received, August 24, 1979;
accepted for publication, November 30, 1979.